

Gravitational radiation from crystalline color-superconducting hybrid stars

Bettina Knippel, Armen Sedrakian

Institute for Theoretical Physics, Goethe-University, D-60438 Frankfurt am Main, Germany

(Dated: September 25, 2018)

The interiors of high mass compact (neutron) stars may contain deconfined quark matter in a crystalline color superconducting (CCS) state. On a basis of microscopic nuclear and quark matter equations of states we explore the internal structure of such stars in general relativity. We find that their stable sequence harbors CCS quark cores with masses $M_{\text{core}} \leq (0.78 - 0.82)M_{\odot}$ and radii $R_{\text{core}} \leq 7$ km. The CCS quark matter can support nonaxisymmetric deformations, because of its finite shear modulus, and can generate gravitational radiation at twice the rotation frequency of the star. Assuming that the CCS core is maximally strained we compute the maximal quadrupole moment it can sustain. The characteristic strain of gravitational wave emission h_0 predicted by our models are compared to the upper limits obtained by the LIGO and GEO 600 detectors. The upper limits are consistent with the breaking strain of CCS matter $\sigma \leq 10^{-4}$ and large pairing gaps $\Delta \sim 50$ MeV, or, alternatively, with $\sigma \sim 10^{-3}$ and small pairing gaps $\Delta \sim 15$ MeV. An observationally determined value of the characteristic strain h_0 can pin down the product $\sigma\Delta^2$. On the theoretical side a better understanding of the breaking strain of CCS matter will be needed to predict reliably the level of the deformation of CCS quark core from first principles.

I. INTRODUCTION

Compact (neutron) stars are important sources of gravitational wave radiation. Gravity waves, to lowest order, arise from time-dependent quadrupole deformations of masses. Rotating, isolated compact stars will emit gravitational radiation if their mass distribution is nonaxisymmetric with respect to their rotation axis. The axial symmetry can be broken over detectable time-scales in a number of ways, e. g., through distortions in the solid phases of the star [1, 2, 3, 4, 5, 6, 7], deformations caused by strong magnetic fields [8, 9, 10, 11, 12], or by precession [13, 14, 15, 16, 17]. Continuous gravitational waves emitted by nonaxisymmetric rotating compact stars are expected to be in the bandwidth of current gravitational wave interferometric detectors. Upper limits on the strain of gravitational waves from a large selection of known radio pulsars were set recently by the LIGO Collaboration under the assumption that the radiation is at twice the pulsar spin frequency [18]. Ellipticities derived from these upper limits are within a range that is compatible with theoretical predictions. Current data from the fifth LIGO science run places upper limits on the gravitational wave amplitude from the Crab pulsar at $h = 3.4 \times 10^{-25}$ (95% confidence), which is below the spin-down limit (i.e., the limit obtained assuming that all the energy loss is due to gravitational radiation) by a factor of 4 [19].

In this work we study gravitational wave emission from compact stars featuring a crystalline color-superconducting (CCS) phase of quark matter in their interiors. Our study is based on microscopic equations of state of nuclear and quark matter, described earlier in a study of the integral parameters of nonrotating and rapidly rotating hybrid configurations [20]. The ellipticity of CCS quark stars and the associated gravitational wave emission was estimated earlier for uniform-density incompressible models. On the basis of such a model

Lin [21] concluded that the upper limit for the Crab pulsar provides useful constraints on the QCD parameters. Haskell et al. [22] estimated core deformations and associated with them constraints on the QCD parameters for sequences of $1.4 M_{\odot}$ and $R = 10$ km stars containing CCS quark cores with different transition densities from nuclear to quark matter. The nuclear matter equation of state was approximated by a $n = 1$ polytrope, and quark matter was treated as an incompressible fluid. Equilibrium and stability of hybrid compact stars constructed from microscopic equations of state of quark and nuclear matter were studied in Ref. [20]. For stellar sequences that are based on microscopic input the stability is not a guaranteed feature. The equilibrium among the quark and nuclear phases is achieved for rather stiff nuclear equations of state, while those configurations that contain quark phase(s) often belong to unstable branches of the sequences [23, 24, 25, 26, 27, 28, 29]. For our microscopic input a stable branch of CCS hybrid stars emerges in the form of a “second family” of configurations, which is separated from their purely nuclear counterparts by a region of instability. The masses of the resulting hybrid configurations are close to the maximum sustainable mass $M_{\text{max}} \simeq 2M_{\odot}$, i.e., are much more massive than “canonical” neutron stars with $M \sim 1.4M_{\odot}$.

Below, by resorting to microphysical input we add realism to the treatment of the gravitational radiation from hybrid compact stars, in particular, the constraints on microscopic parameters derived from the observational upper limits. Even though we lift a large portion of uncertainties related to the microphysical input of the theory, the elastic properties of the CCS phase and other solid phases of our models (nuclear crusts) remain uncertain. The breaking strain that solid phases of compact stars can sustain is difficult to compute and is usually assumed to lie in the range $10^{-5} \leq \sigma \leq 10^{-2}$. The values close to the upper “optimistic” bound of σ implies distortions in the star’s crusts and/or core that are interesting

from the perspective of gravitational wave emission. We concentrate below on distortions in the CCS phase and will ignore any other contributions, as those originating from the distortions in the crusts, precession or magnetic deformations. Distortions may exist in other types of compact objects, such as solid strange stars, quark stars, stars with mixed phases of quarks, meson-condensates and hadrons [30, 31, 32, 33]; the problem of gravitational wave emission from such objects is discussed in the literature [34, 35]. Furthermore, we assume that the CCS quark matter is the true ground state of quark matter in some density interval [36, 37, 38, 39, 40, 41, 42, 43] and that the value of the dynamical strange quark mass is small enough to favor the three-flavor variant of this phase [39, 40, 41, 42]. However, among the candidate phases for the ground state of quark matter at intermediate densities, the three-flavor CCS quark phase and its two-flavor counterpart are the only phases that behave as solids (nonzero shear modulus). Therefore, their possible manifestations via gravitational wave emission is unique among the color-superconducting phases.

This paper is organized as follows: In Sec. II we study the equilibrium sequences of nonrotating hybrid compact stars featuring CCS quark cores. We compute the masses, radii, and quadrupole moments of the quark cores of hybrid configurations. Section III discusses the gravitational wave radiation from the CCS quark cores. The experimental upper limits on the strain of gravitational waves from pulsars are compared to the theoretical predictions of our models. Our conclusions are collected in Sec. IV.

II. MODELS OF CCS QUARK STARS

We consider models of hybrid compact stars constructed from zero-temperature microscopic equations of state of nuclear matter described by Dirac-Bruckner-Hartree-Fock (DBHF) theory and quark matter described by the Nambu-Jona-Lasinio model (see also Ref. [20]). The DBHF approach is based on a self-consistent solution of the equation for the in-medium relativistic T matrix and nucleon self-energy starting from a realistic nucleon-nucleon potential. The potential is adjusted to reproduce the nuclear phase shifts and deuteron binding energy. The saturation properties of nuclear matter are well reproduced within DBHF theories. The quark equation of state is derived from the Lagrangian of the Nambu-Jona-Lasinio model. This model is based on the four-quark contact interaction picture, i.e., the gluons are integrated out from the theory. It exhibits the chiral symmetry restoration in quark matter, but lacks confinement. Its coupling constants and momentum cutoff are adjusted to reproduce the meson masses and the pion decay constant in the vacuum. Deconfinement phase transition between the nuclear and quark phases is implemented via a Maxwell construction, i.e., it occurs at the point where the pressures of both phases

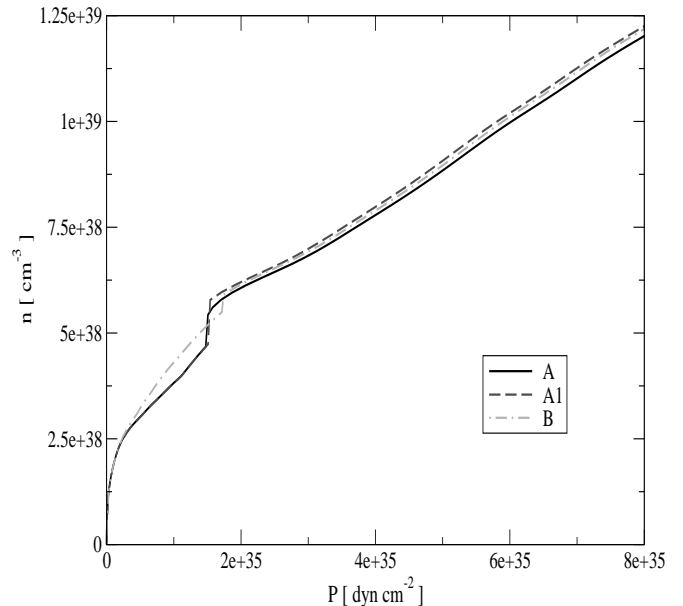


FIG. 1: (Color online) Number density versus pressure for models A (*solid, black online*), A1 (*dashed, red online*), and B (*dashed-dotted, blue online*). For models A and A1 the nuclear (low density) equation of state is the same; for models A and B the quark (high-density) equation of state is the same. At the deconfinement phase transition there is a jump in the density at constant pressure.

as functions of the baryonic chemical potential coincide. At the deconfinement phase transition the density experiences a jump at constant pressure and zero temperature. Within the quark matter phase a Cooper pair condensate of quarks with mismatched Fermi-surfaces will emerge. Our models feature the so-called three-flavor Larkin-Ovchinnikov-Fulde-Ferrell (LOFF) or crystalline color-superconducting (CCS) phase as a possible candidate of the ground state of Cooper-paired quark matter [36, 37, 38, 39, 40, 41, 42, 43]. In this phase the condensate order parameter is spatially modulated; as a result the superfluid phase behaves as a solid with finite shear modulus. This, in turn, implies that the LOFF phase can sustain equilibrium nonaxisymmetrical deformations, which potentially can lead to gravitational wave radiation. It should be noted that a more complete treatment of high-density matter will need to include phases other than the CCS phase and the possibility of transitions between them [44]. However, the latter phases are not crystalline and are unlikely to affect the physics of gravitational wave emission in a direct manner. Indirectly, they may have an effect, e. g., by changing the fractional volume occupied by the CCS phase.

We consider three different equations of state that are displayed in Fig. 1 (see also Fig. 1 of Ref. [20]). For models A and A1 the nuclear (low density) equation of state is the same; for models A and B the quark (high-density) equation of state is the same. At the deconfinement

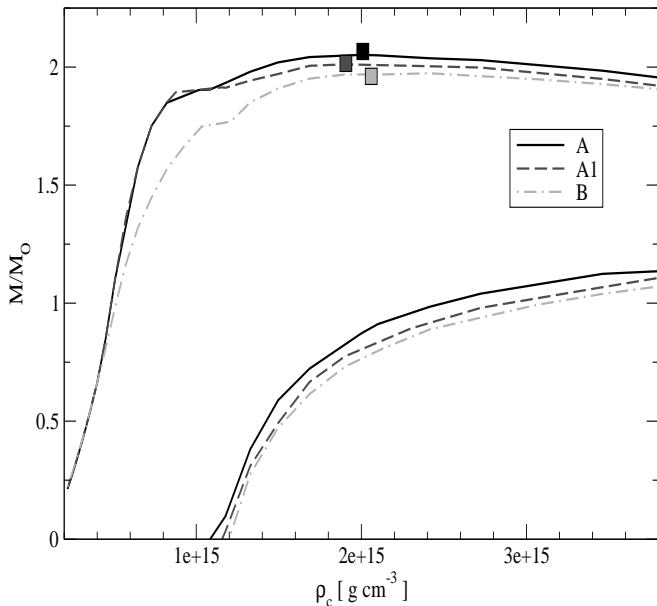


FIG. 2: (Color online) Dependence of the total stellar mass and the mass of the quark core in units of solar mass M_\odot on the central density for nonrotating configurations based on equations of state A, A1, and B (the labeling is as in Fig. 1). The lower set of curves represents the masses of the CCS quark cores, the upper set - the total masses of the configurations. The maximal masses are marked with boxes.

ment phase transition there is a jump in the density at constant pressure. The high-density regime contains two equations of states for crystalline color superconductivity which differ by the normalization of pressure at zero density (bag constant). Model A1 is normalized such that the pressure vanishes at zero density. For models A and B the zero density pressure is shifted by amount $\delta p = 10 \text{ MeV}/\text{fm}^3$. The quark condensate is assumed to be in the strong coupling regime, where the ratio of the couplings in the quark-quark and quark-antiquark channels $\eta = 1$ (the “canonical” value is $\eta = 0.75$ and follows from the Fierz transformation from the quark-anti-quark to quark-quark channel.) The values of the (baryonic) chemical potential (in MeV) and pressure (in MeV/fm^3) at the quark-nuclear matter interface are (1234.2; 96) for model A1, (1230.0; 95) for model A and (1234.8; 108) for model B [20]. We start by considering the equilibrium and stability of nonrotating cold hybrid stars with crystalline color-superconducting cores. Our emphasis will be on the internal structure and the integral parameters (mass, radius, etc) of the quark cores, rather than the integral parameters of the stars (these are discussed in Ref. [20]). We parameterize the sequences of equilibrium, nonrotating stellar configurations in general relativity in terms of the central density ρ_c of the configuration. It is assumed that the configurations are cold, i.e., the stellar structure does not depend on temperature. (Because of large magnitudes of gaps, color-superconducting

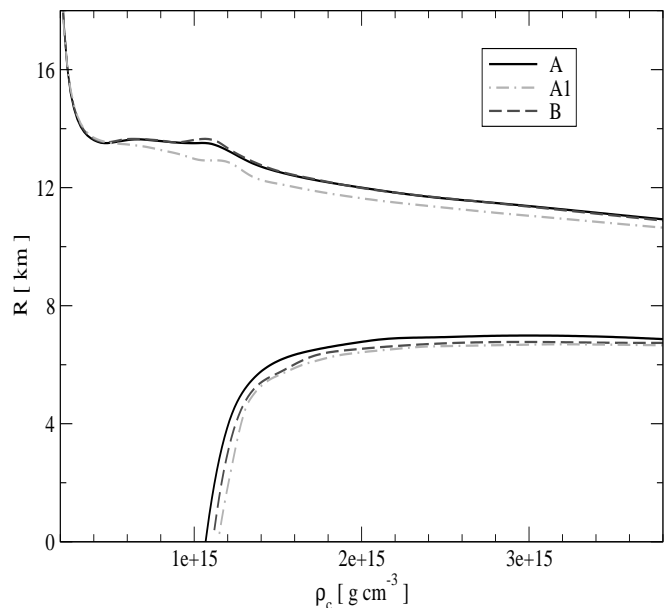


FIG. 3: (Color online) Dependence of radii of nonrotating compact stars and the radii of their quark cores on central density for models A, A1, and B (the labeling is the same as in Fig. 1). The lower set of curves represents the radii of the CCS quark cores, the upper set the radii of the configurations.

phases can affect the early thermal evolution of neutron stars; we assume that our models have cooled down to temperatures well below the respective Fermi energies [45, 46, 47]). We obtain the spherically symmetric solutions of Einstein’s equations for self-gravitating fluids by solving the well-known Tolman-Oppenheimer-Volkoff equations [48]. A sequence of configurations is stable if the derivative $dM/d\rho_c$ is positive, i.e., the mass is an increasing function of the central density. At the point of instability the fundamental (pulsation) modes become unstable. If the stability is regained at higher central densities the modes by which the stars become unstable toward the collapse belong to higher order harmonics.

The masses of the stellar configurations (M) and the CCS quark cores (M_{core}) as a function of the central density are shown in Fig. 2. The sequences of hybrid configurations ($M_{\text{core}} > 0$) appear with increasing central density when the density of deconfinement phase transition is reached. Prior to that point the stars are purely nuclear and become unstable ($dM/d\rho_c \leq 0$) before the stability is regained by the hybrid configurations. The masses of this “second family” vary in a narrow range around the maxim attainable mass $2M_\odot$, which is reached at the central density $2 \times 10^{15} \text{ g cm}^{-3}$. The values of the maximum masses are large as a consequence of the hardness of the underlying nuclear equations of state. The masses of the CCS quark cores cover the range $0 \leq M_{\text{core}}/M_\odot \leq 0.75 - 0.88$ for central densities $1.3 \times 10^{15} \leq \rho_c \leq 2 \times 10^{15}$. Thus, the quark core mass ranges from one third to about the half of the total

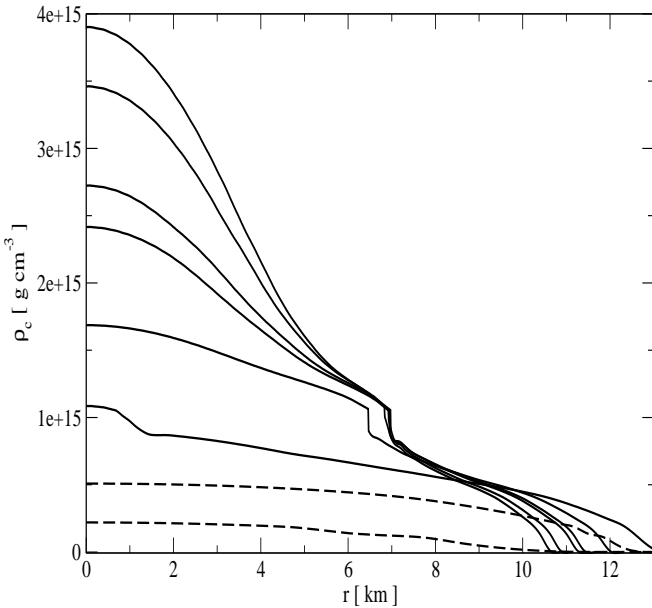


FIG. 4: Dependence of density on the internal radius for model A. The dashed lines correspond to purely nuclear stars, the solid lines to hybrid configurations. For latter models there is a density jump at the phase transition to quark matter. The transition radius saturates at the value $R_{\text{core}} = 7$ km as the central density is increased.

stellar mass. Above one solar mass quark cores can be harbored only by unstable configurations.

Fig. 3 displays the radii of hybrid configurations along with the radii of the CCS quark cores. With the onset of CCS quark phase the radii of the configurations become smaller, i.e., the hybrid configurations are more compact (and more massive) than their neighboring purely nuclear counterparts. Within their stability range the hybrid configurations have almost constant radii $R = 12$ km. The radius of the quark core increases rapidly with the onset of the quark phase and saturates at the asymptotic value $R_{\text{core}} = 7$ km. The quark cores occupy about 20% of the volume of the star. The density profiles of configurations are displayed in Fig. 4. For purely nuclear configurations the density profile is flat in the core. As the central density exceeds the deconfinement transition density, the profiles show a density jump at some internal radius. The jump reflects the behavior of the equation of state at the deconfinement phase transition. There is a rapid growth of the radius (volume) of the quark phase as the density is increased from 1.3×10^{15} to 1.6×10^{15} g cm^{-3} . For larger central densities, i.e., more massive objects, the radius at which the transition from quark to nuclear matter takes place is independent of the central density of the configuration (see also Fig. 3).

Figure 5 displays the mass-radius (M - R) relationship for the stellar configurations (right set of curves) and the CCS quark core (the left set of curves) for models A, A1, and B. The M - R diagram for the stellar con-

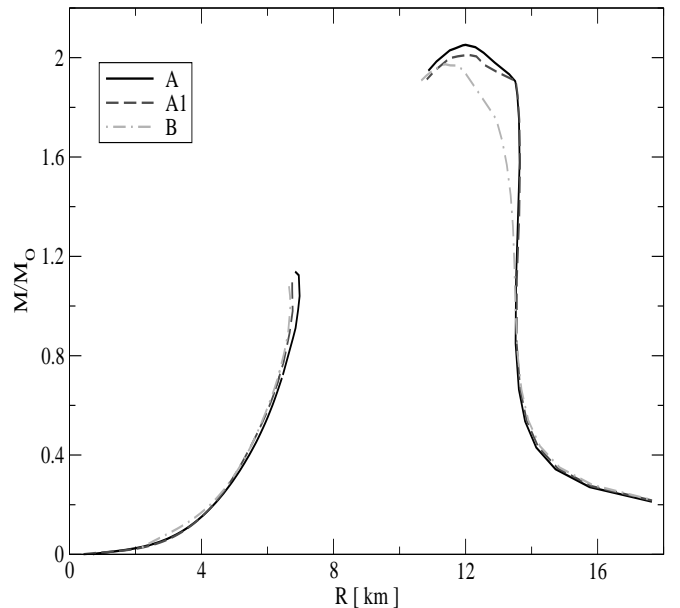


FIG. 5: (Color online) Mass-radius relationship for hybrid stars for models A, A1, and B (the labeling is as in Fig. 1). The right set corresponds to the stellar configurations, the left set to the CCS quark cores.

figurations has been discussed elsewhere [20]; we recall that the obtained mass-radius relationships are consistent with the current astronomical bounds on neutron star masses. They are consistent with the line in the M - R diagram inferred from EXO0748-676 [49]. Note that the emission of redshifted lines used to put constraints in Ref. [49] has not been confirmed in a subsequent observation of Ref. [50]. Also note that alternative models of quark stars are consistent with these bounds, which therefore do not rule out the hypothesis of quark matter in compact stars [51]. The M - R tracks for the CCS quark core display the rapid increase in the radius of the core in the presence of the small amount of quark matter [the $M(R)$ slope is almost horizontal to the R -axis]. The maximal masses of quark cores of the stable configurations are in the range $M \leq 0.75 - 0.88 M_{\odot}$ depending on the equation of state; cores with larger masses correspond to configurations that are unstable toward collapse into a black hole.

III. QUADRUPOLE MOMENTS AND GRAVITATIONAL WAVE EMISSION

The characteristic strain amplitude of gravitational waves emitted by a triaxial star rotating about its principal axis is

$$h_0 = \frac{16\pi^2 G}{c^4} \frac{\epsilon I_{zz} \nu^2}{r}, \quad (1)$$

where ν is the star's rotation frequency, r is the distance to the observer, $\epsilon = (I_{xx} - I_{yy})/I_{zz}$ is the equatorial ellipticity, I_{ij} is the tensor of moment of inertia, G is the gravitational constant, c is the speed of light. The characteristic amplitude, Eq. (1), does not involve the orientation of the source with respect to the observer; it is related to the sources' angle averaged field strength $\langle h^2 \rangle = \int d\Omega (h_+^2 + h_\times^2)/4\pi$ by the relation $h_0 \simeq 1.15 \langle h^2 \rangle$. Alternatively, the strain amplitude can be expressed in terms of the $m = 2$ mass quadrupole moment as

$$h_0 = \frac{16\pi^2 G}{c^4} \left(\frac{32\pi}{15} \right)^{1/2} \frac{Q_{22} \nu^2}{r}, \quad (2)$$

where the mass multipole is defined as $Q_{lm} = \int \rho r^l Y_{lm}^* d^3r$. Thus, to compute the characteristic strain amplitude of gravitational waves we need to compute the quadrupole moment of a CCS quark core in static equilibrium. The elastic deformations are assumed to be small perturbation on the background equilibrium of the star; the equilibrium between gravity and elastic forces, in the Cowling approximation, implies that [7]

$$\nabla^i \delta \tau_{ij} = \delta \rho g(r) \hat{r}_j, \quad (3)$$

where $g(r)$ is the local gravitational acceleration, δ represents Eulerian perturbation, $\tau_{ij} = -pg_{ij} + t_{ij}$ is the stress-energy tensor of the CCS phase, t_{ij} is the shear stress tensor, and g_{ij} is the flat 3-metric (indices i and j run over 1,2,3). Upon expanding the tensor t_{ij} in spherical harmonics and integrating (3) with the boundary condition that assumes vanishing stress in the nuclear envelope surrounding the CCS quark core one finds [cf. Ref. [7], Eq. (64)]

$$Q_{22} = \int_0^{R_{\text{core}}} \frac{dr r^3}{g(r)} \left[\frac{3}{2}(4-U)t_{rr} + \frac{1}{3}(6-U)t_\Lambda + \sqrt{\frac{3}{2}} \left(8 - 3U + \frac{1}{3}U^2 - \frac{r}{3} \frac{dU}{dr} \right) t_{r\perp} \right], \quad (4)$$

where $U = 2 + d \ln g(r) / d \ln r$ and t_{rr} , t_Λ and $t_{r\perp}$ are the coefficients of the expansion of the shear stress tensor in spherical harmonics [7]. These (unknown) coefficients can be determined if one assumes that the CCS core is maximally strained. The shear modulus is defined as $\mu = t_{ij} / 2\sigma_{ij}$, where σ_{ij} is the strain tensor. The shear modulus of CCS matter has been estimated in Ref. [42]

$$\mu = 2.47 \text{ MeV fm}^{-3} \left(\frac{\Delta}{10 \text{ MeV}} \right)^2 \left(\frac{\mu_q}{400 \text{ MeV}} \right)^2, \quad (5)$$

where Δ is the gap parameter, μ_q is the quark chemical potential. For a maximally strained CCS core

$$\begin{aligned} t_{rr} &= 2\mu \left(\frac{32\pi}{15} \right)^{1/2} \bar{\sigma}_{\text{max}}, & t_{r\perp} &= 2\mu \left(\frac{16\pi}{5} \right)^{1/2} \bar{\sigma}_{\text{max}}, \\ t_\Lambda &= 2\mu \left(\frac{96\pi}{5} \right)^{1/2} \bar{\sigma}_{\text{max}}, \end{aligned} \quad (6)$$

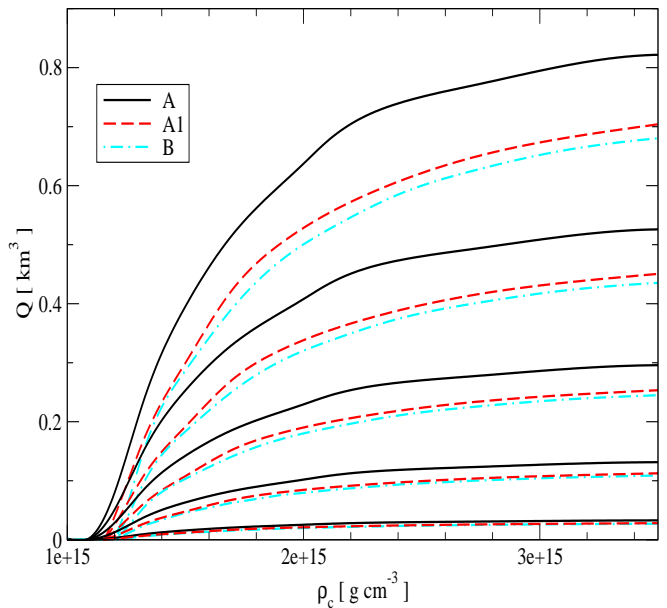


FIG. 6: (Color online) The quadrupole moments of stellar configurations computed according to Eqs. (4), (5) and (6) for models A, A1, and B as a function of central density (the labeling of models is as in Fig. 1). Each triple of curves corresponds to the gap parameter value (from top to bottom) $\Delta = 50, 40, 30, 20,$ and 10 MeV. The magnitude of the breaking strain is $\bar{\sigma}_{\text{max}} = 10^{-2}$, and Q_{max} scales linearly with $\bar{\sigma}_{\text{max}}$.

where $\bar{\sigma}_{\text{max}}$ is the maximal value of the quantity $\bar{\sigma}^2 = \sigma_{ij} \sigma^{ij} / 2$ (breaking strain). It is assumed that the strain in the CCS core is position independent. By combining Eq. (4) and (6) we obtain the maximal quadrupole moment Q_{max} . If the core is uniform and incompressible, then [35]

$$\tilde{Q}_{\text{max}} \simeq \frac{13\mu \bar{\sigma}_{\text{max}} R_{\text{core}}^6}{GM_{\text{core}}}. \quad (7)$$

Figure 6 displays maximal quadrupole moments of a sequences of hybrid stars derived by combining Eqs. (4), (5) and (6). The quadrupole moment depends on the product of the breaking strain and the shear modulus. The former will be treated as a free parameter in view of the poor knowledge of this quantity; in Fig. 6 we assume $\bar{\sigma}_{\text{max}} = 10^{-2}$. Since the equation of state fixes the quark chemical potential, the only parameter on which the shear modulus depends is the gap, which we will vary in the range $10 \leq \Delta \leq 50$ MeV. It is assumed that the gap is independent of the density of the CCS quark phase. Treatments of the CCS phase that are based on the Ginzburg-Landau expansion near the critical temperature predict values of gaps that are in the range $5 \leq \Delta \leq 25$ MeV. The low temperature CCS phase (more relevant for the problem at hand) is likely to support a larger, up to 100 MeV, gap. The maximal quadrupole moment scales as $Q_{\text{max}} \sim \bar{\sigma}_{\text{max}} \Delta^2$ according to Eqs. (4)–(6).

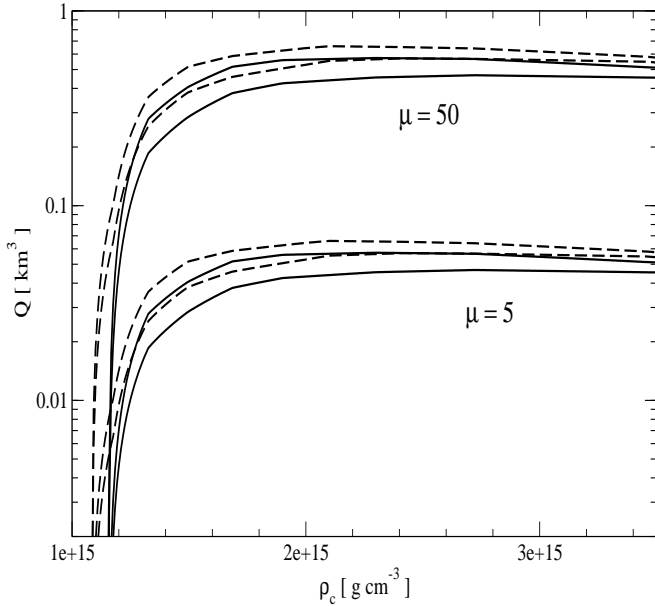


FIG. 7: The quadrupole moments of stellar configurations (solid lines) computed for fixed values of the shear modulus of CCS quark matter $\mu = 5$ and $\mu = 50$ MeV fm $^{-3}$ for model A as a function of central density. The dashed lines represent the uniform-density incompressible matter approximation, Eq. (7), where the masses and radii are set equal to that of the quark cores of microscopic models (the values of the central densities on the x axis do not represent the central densities of these models).

Figure 7 compares the quadrupole moments of quark cores of stellar configurations computed from the microscopic equations of state A, A1, and B with the quadrupole moments of uniform, incompressible objects computed via Eq. (7). The masses and radii of the latter are set equal to that of the quark cores in the microscopic models. (Note that the central densities on the abscissa of Fig. 7 refer only to the microscopic models.) It is seen that the uniform, incompressible approximation systematically overestimates the magnitudes of the quadrupole moments, although numerically the error is not large. An accurate value of the quark core radius, that follows from our microscopic treatment, appears to be a more important factor in providing realistic values of Q_{\max} because of $Q_{\max} \sim R_{\text{core}}^6$ scaling.

Figure 8 displays the strain of gravitational wave emission given by Eq. (2) for models A, A1, and B as a function of the core mass M_{core} (the results for model A overlap with that of model B on the scale of the figure). Each pair of curves corresponds to the gap parameter value (from top to bottom) $\Delta = 50, 40, 30, 20,$ and 10 MeV. We assume rotation at the frequency of the Crab pulsar $\nu = 29.6$ Hz at a distance of 2 kpc. Since h_0 is a linear function of quadrupole moment Q_{\max} , its dependence on the gap function reflects the quadratic dependence of Q_{\max} on the gap function discussed above. The

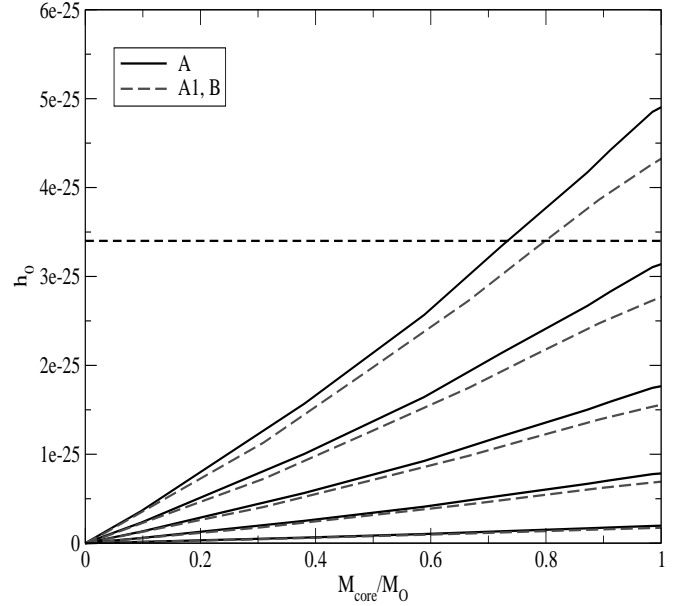


FIG. 8: (Color online) The strain of gravitational wave emission for a pulsar rotating at the Crab pulsar frequency $\nu = 29.6$ Hz at a distance of 2 kpc, computed according to Eqs. (4) and (5) for models A and A1 (the results for models A1 and B overlap on the scale of this figure). Each triple of curves corresponds to the gap parameter value (from top to bottom) $\Delta = 50, 40, 30, 20,$ and 10 MeV. The magnitude of the breaking strain is $\bar{\sigma}_{\max} = 10^{-4}$, and h_0 scales linearly with $\bar{\sigma}_{\max}$. The current upper limit on the strain of the Crab pulsar derived by the LIGO experiment is shown by the horizontal dashed line.

magnitude of the breaking strain is $\bar{\sigma}_{\max} = 10^{-4}$. The current upper limit on the characteristic strain of gravitational radiation from the Crab pulsar is 3.4×10^{-25} and is shown in Fig. 8 by the horizontal dashed line. It is seen that the strain of gravitational wave emission is close to the upper limit for $\Delta = 50$ MeV. If, however, the gaps are small more “optimistic” values of $10^{-3} \leq \bar{\sigma}_{\max} \leq 10^{-2}$ will be needed to generate sizeable strain amplitude. Clearly, because of the large uncertainty in the actual value of $\bar{\sigma}_{\max}$ no definite conclusion can be drawn about the microscopic parameters of the CCS phase from the current upper limits on the strain of gravitational wave emission. The current upper limit for gravitational waves from the Crab pulsar implies $\bar{\sigma}_{\max} \Delta^2 \sim 0.25$ MeV 2 (under the assumptions of the present model).

Figure 9 shows the strain of gravitational wave emission h_0 for two approximations to the quadrupole deformations (realistic vs incompressible), discussed above and illustrated in Fig. 7. As in Fig. 7, the masses and radii of incompressible models are set equal to that of the quark cores derived from the microscopic models, i.e., the abscissa of Fig. 9 refers to central density of the microscopic models only. It is seen that the uniform, incompressible approximation systematically overestimates the magnitude of h_0 for all central densities.

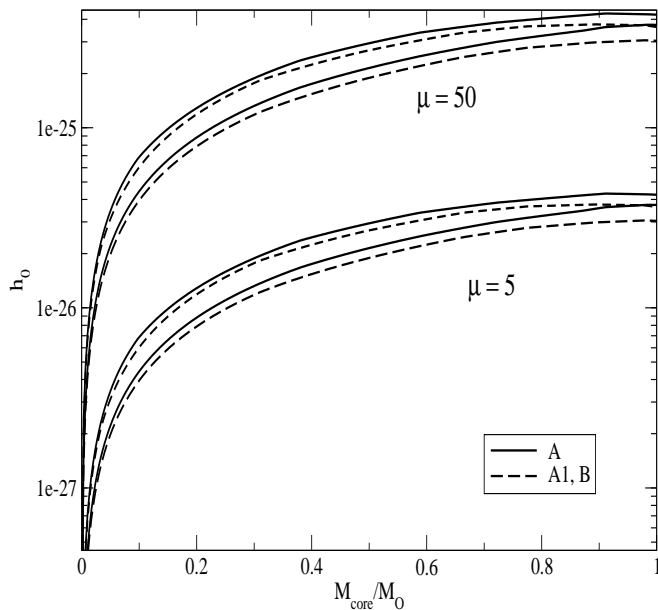


FIG. 9: Same as in Fig. 8, but for fixed values of the shear modulus of CCS quark matter $\mu = 5$ and $\mu = 50$ MeV fm $^{-3}$ for models A (solid lines) and A1 (dashed lines). The results for models A1 and B overlap on the scale of the figure. For each pair of curves with the same value of μ and same equation of state the lower curve is obtained from the full expression for Q_{\max} , while the upper one from the uniform-density incompressible fluid approximation, Eq. (7). The latter approximation systematically overestimates the value of the quadrupole moment. The magnitude of the breaking strain is $\bar{\sigma}_{\max} = 10^{-4}$; h_0 scales linearly with $\bar{\sigma}_{\max}$.

IV. CONCLUSIONS

We studied gravitational wave emission by hybrid compact (neutron) stars harboring maximally strained crystalline color-superconducting quark cores on a basis of microscopic equations of state. In a first step, we (re)constructed hybrid configurations, which are composed of color superconducting quark matter at high and purely nuclear matter at low densities. The high-density quark matter is described in terms of the semimicroscopic Nambu–Jona-Lasinio model which includes pair correlations that lead to the three-flavor LOFF phase as the ground state of QCD at moderate densities. The low density nuclear phase is described in terms of hard relativistic equations of state based on the Dirac-Bruckner-Hartree-Fock theory. These configurations in static grav-

itational equilibrium arise as a “second family” of stable configurations. We find that the stable (with respect to a collapse into a black hole) segment of the sequences have CCS quark cores with masses $0 \leq M_{\text{core}}/M_{\odot} \leq 0.75 - 0.88$ for central densities $1.3 \times 10^{15} \leq \rho_c \leq 2 \times 10^{15}$ and radii up to 7 km. Consequently, about 1/3 of the mass of hybrid configuration is concentrated in its quark core, which occupies about 20 % of star’s volume.

In the second step, we considered the characteristic strain of gravitational wave emission due to deformations of the CCS quark core. If the quark core is maximally strained, the components of the stress tensor can be expressed through product of the breaking strain and the shear modulus of the CCS quark matter. The quadrupole moment and the characteristic strain mainly depend on the not-well-known product $\bar{\sigma}_{\max} \Delta^2$. The current upper limits imply that $\bar{\sigma}_{\max} \Delta^2 \leq 0.25$ MeV 2 , which can be accommodated by assuming either large gaps $\Delta \sim 50$ MeV and moderate values of $\bar{\sigma}_{\max} \sim 10^{-4}$ or small gaps ~ 15 MeV and more “optimistic” values of breaking strain, $\bar{\sigma}_{\max} \sim 10^{-3}$. In view of large uncertainty in the value of breaking strain $10^{-5} \leq \bar{\sigma}_{\max} \leq 10^{-2}$ no definite conclusions can be made about the possible magnitude of the gap in the CCS phase. However, if the gaps are large, $\Delta \geq 50$ MeV, the values $\bar{\sigma}_{\max} \geq 10^{-3}$ are excluded by the present scenario of gravitational wave radiation. Note, however, that the assumption that the CCS core is maximally strained may not correspond to the actual situation in compact stars and the evolutionary avenues that may lead to such maximal deformations are not explored yet. One may only speculate that a rapidly spinning pulsar at birth may be triaxially stretched, a deformation that may be preserved within the star after the transition to the crystalline state. Nevertheless, we conclude that the characteristic strain amplitudes of gravitational waves produced by our models are well within the reach of the current gravitational wave detectors for a wide and reasonable range of parameters.

Acknowledgements

We are grateful to Mark Alford, Nils Andersson, Michael Buballa, Nicola Ippolito, Krishna Rajagopal, Luciano Rezzolla, Dirk H. Rischke, Marco Ruggieri, Lars Samueleson, Jürgen Schaffner-Bielich, Fridolin Weber and Graham Woan for useful interactions. This work was supported in part by the Deutsche Forschungsgemeinschaft.

-
- [1] G. Baym and D. Pines, *Ann. Phys.* **66**, 816 (1971).
 [2] B. Carter and H. Quintana, *Ann. Phys.* **95**, 74 (1975).
 [3] T. Strohmayer, H. M. van Horn, S. Ogata, H. Iyetomi, S. Ichimaru, *Astrophys. J.* **375**, 679 (1991).
 [4] C. Cutler, G. Ushomirsky and B. Link, *Astrophys. J.* **588**,

- 975 (2003) arXiv:astro-ph/0210175.
 [5] B. Haskell, D. I. Jones and N. Andersson, *Mon. Not. Roy. Astron. Soc.* **373**, 1423 (2006) [arXiv:astro-ph/0609438].
 [6] N. Chamel and P. Haensel, *Living Rev. Rel.* **11**, 10 (2008) [arXiv:0812.3955 [astro-ph]].

- [7] G. Ushomirsky, C. Cutler and L. Bildsten, *Mon. Not. Roy. Astron. Soc.* **319**, 902 (2000) [arXiv:astro-ph/0001136].
- [8] S. Bonazzola and E.ourgoulhon, *Astron. Astrophys.* **312**, 675 (1996) [arXiv:astro-ph/9602107].
- [9] C. Cutler, *Phys. Rev. D* **66**, 084025 (2002) [arXiv:gr-qc/0206051].
- [10] I. Wasserman, *Mon. Not. Roy. Astron. Soc.* **341**, 1020 (2003).
- [11] T. Akgun and I. Wasserman, *Mon. Not. R. Astron. Soc.* **341**, 1020 (2003) arXiv:0705.2195 [astro-ph].
- [12] B. Haskell, L. Samuelsson, K. Glampedakis and N. Andersson, *Mon. Not. Roy. Astron. Soc.* **385**, 531 (2008) [arXiv:0705.1780 [astro-ph]].
- [13] M. Zimmermann, *Nature* **271**, 524 (1978); *Phys. Rev. D* **21**, 891 (1980).
- [14] M. A. Alpar and D. Pines, *Nature* **314**, 334 (1985).
- [15] A. Sedrakian, I. Wasserman and J. M. Cordes, *Astrophys. J.* **524**, 341 (1999), arXiv:astro-ph/9801188.
- [16] C. Cutler and D. I. Jones, *Phys. Rev. D* **63**, 024002 (2001) [arXiv:gr-qc/0008021].
- [17] D. I. Jones and N. Andersson, *Mon. Not. R. Astron. Soc.* **331**, 203 (2002), [arXiv:gr-qc/0106094].
- [18] B. Abbott, *et al.* (LIGO Scientific Collaboration) *Phys. Rev. D* **76**, 042001 (2007).
- [19] B. Abbott, *et al.* (LIGO Scientific Collaboration) *Astrophys. J. Letters* **683**, 45 (2008).
- [20] N. Ippolito, M. Ruggieri, D. Rischke, A. Sedrakian and F. Weber, *Phys. Rev. D* **77**, 023004 (2008) [arXiv:0710.3874 [astro-ph]].
- [21] L.-M. Lin, *Phys. Rev. D* **76**, 081502(R) (2007).
- [22] B. Haskell, N. Andersson, D. I. Jones, and L. Samuelsson, *Phys. Rev. Lett.* **99**, 231101 (2007).
- [23] M. Buballa, F. Neumann, M. Oertel and I. Shovkovy, *Phys. Lett. B* **595**, 36 (2004) [arXiv:nucl-th/0312078].
- [24] M. Baldo, M. Buballa, F. Burgio, F. Neumann, M. Oertel and H. J. Schulze, *Phys. Lett. B* **562**, 153 (2003) [arXiv:nucl-th/0212096].
- [25] C. Q. Ma and C. Y. Gao, *Eur. Phys. J. A* **34**, 153 (2007) [arXiv:0706.3243 [astro-ph]].
- [26] G. Pagliara and J. Schaffner-Bielich, *Phys. Rev. D* **77**, 063004 (2008) [arXiv:0711.1119 [astro-ph]].
- [27] H. Grigorian, D. Blaschke and D. N. Aguilera, *Phys. Rev. C* **69**, 065802 (2004);
- [28] D. B. Blaschke, D. Gomez Dumm, A. G. Grunfeld, T. Klahn and N. N. Scoccola, *Phys. Rev. C* **75**, 065804 (2007). [arXiv:nucl-th/0703088].
- [29] M. Alford and S. Reddy *Astrophys. J.* **629**, 969 (2005) [arXiv:nucl-th/0411016].
- [30] F. Weber, *Pulsars as astrophysical laboratories for nuclear and particle physics*, Bristol, U.K.: Institute of Physics, 1999.
- [31] A. Sedrakian, *Prog. Part. Nucl. Phys.* **58**, 168 (2007) [arXiv:nucl-th/0601086].
- [32] G. E. Brown, C. H. Lee and M. Rho, *Phys. Rev. Lett.* **101**, 091101 (2008) [arXiv:0802.2997 [hep-ph]].
- [33] D. Blaschke, T. Klahn and F. Weber, arXiv:0808.1279 [astro-ph].
- [34] R. X. Xu, *Astrophys. J.* **596**, L59 (2003).
- [35] B. J. Owen, *Phys. Rev. Lett.* **95**, 211101 (2005).
- [36] M. G. Alford, J. A. Bowers and K. Rajagopal, *Phys. Rev. D* **63**, 074016 (2001) [arXiv:hep-ph/0008208].
- [37] J. A. Bowers and K. Rajagopal, *Phys. Rev. D* **66**, 065002 (2002) [arXiv:hep-ph/0204079].
- [38] O. Kiriya, D. H. Rischke and I. A. Shovkovy, *Phys. Lett. B* **643**, 331 (2006) [arXiv:hep-ph/0606030].
- [39] R. Casalbuoni, R. Gatto, N. Ippolito, G. Nardulli and M. Ruggieri, *Phys. Lett. B* **627**, 89 (2005) [Erratum-ibid. *B* **634**, 565 (2006)] [arXiv:hep-ph/0507247].
- [40] N. D. Ippolito, G. Nardulli and M. Ruggieri, *JHEP* **0704**, 036 (2007) [arXiv:hep-ph/0701113].
- [41] K. Rajagopal and R. Sharma, *Phys. Rev. D* **74**, 094019 (2006) [arXiv:hep-ph/0605316].
- [42] M. Mannarelli, K. Rajagopal and R. Sharma, *Phys. Rev. D* **73**, 114012 (2006) [arXiv:hep-ph/0603076].
- [43] M. Mannarelli, K. Rajagopal and R. Sharma, *Prog. Theor. Phys. Suppl.* **174**, 39 (2008).
- [44] M. G. Alford, A. Schmitt, K. Rajagopal and T. Schafer, *Rev. Mod. Phys.* **80**, 1455 (2008) [arXiv:0709.4635 [hep-ph]].
- [45] C. Schaab, D. Voskresensky, A. D. Sedrakian, F. Weber and M. K. Weigel, *Astron. Astrophys.* **321**, 591 (1997) [arXiv:astro-ph/9605188].
- [46] H. Grigorian, D. Blaschke and D. Voskresensky, *Phys. Rev. C* **71**, 045801 (2005) [arXiv:astro-ph/0411619].
- [47] D. Page, U. Geppert and F. Weber, *Nucl. Phys. A* **777**, 497 (2006) [arXiv:astro-ph/0508056].
- [48] R. C. Tolman, *Phys. Rev.* **55**, 364 (1939); J. R. Oppenheimer and G. M. Volkoff, *Phys. Rev.* **55**, 374 (1939).
- [49] F. Ozel, *Nature* **441**, (2006) 1115.
- [50] J. Cottam, F. Paerels, M. Mendez, L. Boirin, W. H. G. Lewin, E. Kuulkers, J. M. Miller, *Astrophys. J.* **672**, 504 (2008).
- [51] M. Alford, D. Blaschke, A. Drago, T. Klahn, G. Pagliara and J. Schaffner-Bielich, *Nature* **445**, E7 (2007) [arXiv:astro-ph/0606524].